Title

Studies of Chemisorption with the Scanning Tunneling Microscope

Author

Salmeron, M

Publication Date

1990-10-01

Center for Advanced Materials

CAM

To be published as a chapter in **Lectures on Surface Science II**, Springer-Verlag, Publisher, Berlin, Germany, 1991

Studies of Chemisorption with the Scanning Tunneling Microscope

M. Salmeron

October 1990

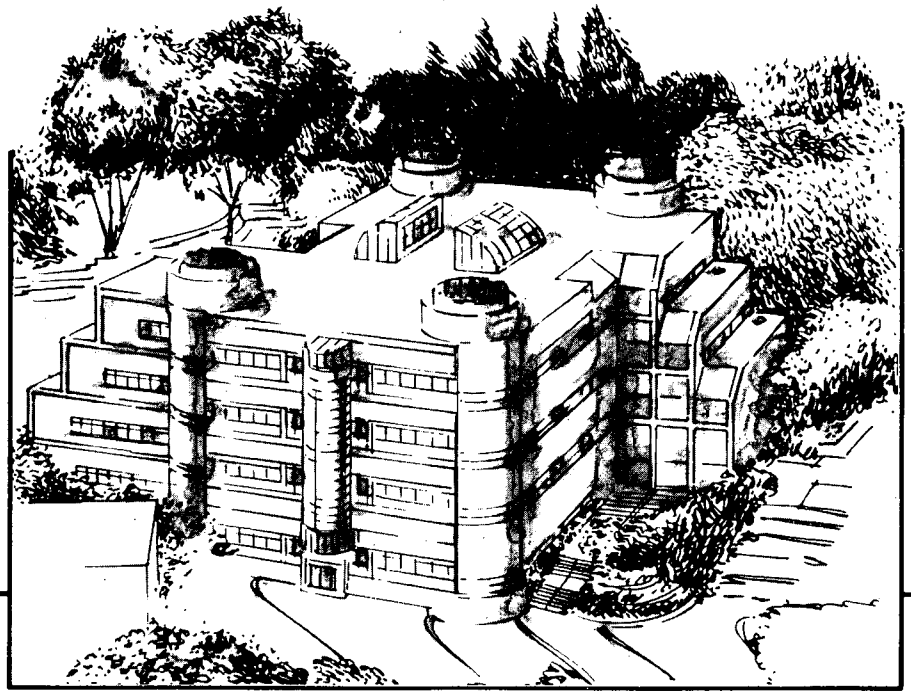

Materials and Chemical Sciences Division

Lawrence Berkeley Laboratory • University of California

ONE CYCLOTRON ROAD, BERKELEY, CA 94720 • (415) 486-4755

Prepared for the U.S. Department of Energy under Contract DE-AC03-76SF00098

DISCLAIMER

LBL 29747

Studies of Chemisorption with the Scanning Tunneling Microscope

M. Salmeron

Center for Advanced Materials
Materials Science Division
Lawrence Berkeley Laboratory
University of California
Berkeley, CA 94720, U.S.A.

October, 1990

This work was supported by the Director, Office of Energy Research, Office of Basic Energy Sciences, Material Sciences Division, U.S. Department of Energy under contract No. DE-AC03-76SF00098.

Studies of Chemisorption with the Scanning Tunneling Microscope

M. Salmeron

Center for Advanced Materials; Materials Science Division
Lawrence Berkeley Laboratory; 1 Cyclotron Road; Berkeley, CA 94720, U.S.A.

Abstract. In this paper we review recent advances in the study of the structure of chemisorbed layers on transition metal surfaces in real space using the Scanning Tunneling Microscope (STM). The examples include Carbon on Pt(111) and Sulfur on Mo(001) and on Re(0001). The new phenomena that were unraveled by the STM and other surface science techniques include the passivation of the surfaces by a single layer of adsorbates that prevented oxidation and contamination in air. In Ultra High Vacuum, the STM revealed the multiple structures formed by S on Re as a function of coverage. It revealed also that at local coverages above 0.25 monolayers, isolated S adatoms are not stable and coalesce into structures formed by trimers and other aggregates.

1. Introduction

The scanning tunnelling microscope (STM) has made it possible to study in real space the atomic structure of surfaces of metals and semiconductors [1]. One area that is particularly relevant to epitaxy and catalysis is that of the crystallographic structure of surface layers. Until recently, this has been studied mostly with low energy electron diffraction (LEED) [2].

LEED, as all diffraction techniques, is sensitive to the ordered areas of the surface while the defect structures (steps, domain boundaries, point defects, etc.) are not easily detected. However, these defect structures are thought to play a major role both in crystal growth and in catalysis [3].

In addition to providing local atomic structure information, the STM is capable of operating in a wide range of environments, including ultra high vacuum, liquids, and atmospheric.

In this paper we will show how the STM has been applied in the author's laboratory to unravel the structure of carbon layers on platinum and sulphur layers on molybdenum and rhenium single crystals. One outcome of these studies is the observation of multiple defect structures that could not be observed by LEED before and also of new phenomena like the coalescence of adsorbate atoms into clusters in disordered and ordered arrangements. While the ordered structures are in principle resolvable by diffraction methods, the size of the new unit cell is often too large for present day computational programs.

2. Principle of STM Operation

The STM is based on the measurement and control of the tunneling current between a sharp metal tip (W and Pt-Rh alloys in these studies) and a conductive surface. The electrons "tunnel" through the potential barrier between tip and surface. The height of this barrier is derived from the work function of the two materials. The tunnel current therefore depends exponentially on both the tip surface distance (z) and the barrier height Ø through:

$$I \alpha e^{-\sqrt{\phi}.z}$$

The exponential dependence of the tunneling current I on the distance z is the basis for the high spatial resolution of the STM in the direction perpendicular to the surface z. This resolution is limited by noise to a typical value of 0.1 Å.

The sharpness of the tip determines the "in-plane" resolution. This is provided by natural asperities at the apex of tips that often terminate in one or a few atoms. Because of the exponential decay of I with z, the atomic size asperity that is closest to the surface will carry most of the tunnel current I. The fine displacements of the tip over the surface are controlled by a piezoelectric transducer that is capable of fine displacements of the order of 10 Å per applied volt. A schematic of the experimental set up is shown in figure 1.

Because of the nature of this paper, we will not describe many important experimental details, including isolation from mechanical and other electric perturbations, approach of tip to sample from macroscopic (1 cm typically) to microscopic distances (5 to 10 Å), and others. The interested reader might consult several reviews on those subjects [4,5].

The images are formed by a three-dimensional plot of x, y, and z coordinates obtained by scanning the tip over the surface while maintaining the tunnel current I constant.

3. Carbon on Pt(111)

The first system that we present is the monolayer formed by C on Pt(111). This system is important in hydrocarbon catalysis since it is the by-product from many reactions after high temperature (larger than 300° C treatments). In the present experiments, the carbon overlayer was obtained by heating in ultra high vacuum (UHV) a hydrocarbon contaminated Pt(111) crystal. After heating, the sample was analyzed by Auger Electron Spectroscopy (AES) and LEED. Our AES calibration indicated that carbon coverage θ was 1 monolayer on the average and LEED indicated the presence of rings in the diffraction pattern characteristic of graphite [4]. Then the sample was placed in the STM located in the same UHV chamber and imaged. Large terraces and multi- atom height steps were observed over the whole surface. At the atomic scale, the images clearly revealed the graphitic nature of the carbon layers as shown in figure 2. The higher density of valence electronic states in the regions between carbon atoms is clearly observed as elevations in the current image. In this image we observe also that the distribution of tunneling current intensity is not six-fold symmetric, as expected from the honeycomb lattice of a single graphite layer, but rather three-fold symmetric. Some authors have proposed that such distribution, that is also observed in graphite crystals, is due to an electronic interaction between first and second carbon layers. Our observation of three-fold symmetry can then be due to a local coverage of carbon of two monolayers in spite of the AES observation of one monolayer average coverage over mm^2 areas.

The results are revealing both of the power of STM as a local probe and also of its limitations. The very small area examined (a few tens of Angstroms with atomic resolution) might not be representative of the average surface structure. Further experiments on this system are needed to insure that the area imaged is one carbon layer thick. One way to ascertain this is by finding a region consisting of an island of graphite where the substrate outside it is also imaged. One additional observation on this system was the stability of the C structure to air exposure. The images obtained immediately after extracting the crystal from the UHV chamber revealed the graphitic structure still present in air.

4. Sulphur on Mo(100)

Sulphur overlayers on molybdenum single crystals have been studied in the past by LEED [6,7]. This system is interesting because it was shown that its chemical activity in hydrodesulphurization (HDS) reactions parallels that of the industrial catalyst based on promoted MoS_2. In many basic surface science studies of model catalysts, a host of surface science techniques are used to

characterize the state of the catalyst surface before (in UHV) and after the reaction. Since this reaction takes place in an environmental cell, no characterization is done during the reaction at high pressure (≥1 torr) and high temperature (> 200° C). One of the main open questions in catalysis science is how the structure of the catalyst surface is modified by the presence of the reactants. The solution to that question is to develop techniques that can reveal the atomic structure of the catalyst in high pressure environments. The STM is one possible answer. With this aim in mind, a special version of this instrument is being developed in the author's laboratory that will operate at high reactant pressure and at high temperatures of up to 200° C. As a test to investigate whether the STM can resolve the atomic structure of chemisorbed layers at high pressure we have studied the structure of a passivating monolayer of sulphur on Mo(001) [8]. This layer was prepared in UHV and characterized by LEED and Auger. Then it was studied by STM after transfer of the crystal to atmospheric environments. We found that S protects the surface from oxidation in air as checked by LEED and AES after reinsertion of the crystal in the UHV chamber. This passivating layer corresponds to the saturation coverage (1 S atom per surface Mo atom). Its structure has a periodicity of (1x2) which means that the new surface lattice has 1 times and 2 times the dimensions of the clean Mo(100) surface along each unit cell vector.

The STM images obtained revealed the atomic structure of this overlayer as shown in figure 3. The unit cell is indicated by the rectangle. As we can see, the sulphur atomic arrangement is a compact pseudohexagonal lattice with sulphur-sulphur distances of 3.1 Å. This is the short side of the rectangular cell. This distance is comparable to the 3.16 Å found in the basal planes of molybdenum disulfide (MoS_2). The compactness of this pseudohexagonal layer and the strong binding of S to Mo are responsible for the passivating properties that S imparts to the surface towards contamination and oxidation. The oxide is thermodynamically more stable than the sulphide. However, to initiate the oxidation of the surface, a pair of exposed nearest Mo sites are required where the O_2 molecule can dissociate. These sites are not available on the perfect S overlayer structure. The oxide formation is therefore retarded by a kinetic barrier. After prolonged exposure to the atmosphere, eventually the oxide nucleates at defects and expands to the whole surface, displacing the S. The time scale for this process is variable since it is controlled by the number of defects. This depends in turn on the preparation conditions. One example of surface oxide formed after three days of exposure to air is shown in figure 4. The oxide crystallites grow as elongated rectangles along the two principal crystallographic directions and have an average size of 20 x 60 Å.

These results are important because they showed for the first time that high pressure environments--in this case 1 atmosphere of O_2 and N_2 and other gases found in air, do not prevent the operation of the STM and chemisorbed layers can still be imaged with atomic resolution.

Further details on the S structure found with the STM are described elsewhere [8,9].

5. Sulfur on Re(0001)

The structures formed by sulphur on Re(0001) surfaces as a function of coverage θ, have been studied by LEED and AES [10]. Recently [10], STM was applied to study the structure of the saturation coverage layer at θ = 0.50. At saturation S imparts to the Re(0001) surface similar passivating properties as in the previous example of Mo(001). To study the structures formed at lower coverage, the experiments have to be performed in UHV. We have recently completed studies of the structures formed from around θ = 0.25 up to θ = 0.50 [12,13]. The outcome of these studies constitute a dramatic demonstration of how STM helps solve structures with large unit cells. The capability to study complicated structures is not only an incremental refinement of crystallographic techniques, but it allows to uncover new phenomena, like new phases formed by adsorbate aggregation. We describe now briefly these findings. Up to a coverage of 0.25, S-S repulsive pairwise interactions dominates the structure of the absorbed layers. The two structures

observed, the c($\sqrt{3}$ x 5)Rect and the (2x2) conform to the rule of maximum spreading of the S adatoms. As the coverage increases, S-S distances would be maximized and energy minimized by forming structures like the ($\sqrt{3}$x$\sqrt{3}$)R30 when θ = 0.33, as observed on many other single crystal surfaces [14,15]. Instead, on Re(0001) a new phase forms in which S coalesces into trimers, first near domain boundaries and then at all regions as shown in figure 5. In these trimers, each sulphur atom sits on the same three-fold hollow site as in the low coverage monomer structures. The fact that dimers do not form except as occasional defects indicates that three-body forces are determinant at this stage. Three body forces were previously introduced as necessary corrections to the dominant pairwise interactions in Monte Carlo simulations of gas lattice dynamics in order to fit the experimental data [16]. Here, these forces are dominant and cause the local coverage to change abruptly from 0.25 to near 0.45 (the value for the ordered ($3\sqrt{3}$x$3\sqrt{3}$)R30° structure described below.) Initially, the trimers are identical and have their center on a three-fold hollow site. As the coverage continues to increase, trimers of a different structure form that are rotated 60° relative to the first ones and have their center on a top site. At maximum trimer density an ordered ($3\sqrt{3}$x$3\sqrt{3}$)R30° structure forms that is composed of trimers of the two types in a 3 to 1 ratio, as shown in figure 6. Atom counting indicates that the coverage is 0.45. By adding more sulphur to the surface, the trimers incorporate a fourth sulphur atom to form tetrameres in a transformation requiring little surface rearrangement. The image of figure 7 shows the new structure formed at completion, a (3,1;1,3) in LEED mattrix notation. Notice the asymmetry of intensity of tunnel current at the sulphur atoms in the tetrameres. It reflects the reduced substrate symmetry with only one mirror plane. The coverage, determined by counting atoms, is 0.5. This observation came also as a surprise. The highest coverage structure (and saturation) was thought to be the one obtained by further dosing, with a structure of($2\sqrt{3}$x$2\sqrt{3}$)R30°, where S forms hexagonal units as shown in figure 8. The coverage here is again 0.5. To form this last structure, a higher exposure to H_2S or S_2 is required. By heating this saturation structure to increasingly higher temperatures, all the lower coverage ones can be generated, including the tetrameres that coexist with the trimers and defects. The ($2\sqrt{3}$x$2\sqrt{3}$)R30° structure might be energetically more stable than the (3,1;1,3), but it requires a substantial rearrangement of sulphur atoms in order to break the trimer unit. Thus the tetrameres structure is kinetically stabilized against the more stable hexagonal ring structure.

6. Conclusions

The examples presented in the previous sections are representative of the qualitative and quantitative change in our understanding of surface structure and phenomena brought about by the application of the STM. We believe that the application of STM and probably also AFM, the Atomic Force Microscope not discussed in this paper, to studies of catalyst surfaces under realistic conditions of pressure and temperature, will bring similar or perhaps even more dramatic changes to our understanding of catalyst structure and operation.

Acknowledgments

This work was supported by the Director, Office of Energy Research, Office of Basic Energy Sciences, Material Sciences Division, U.S. Department of Energy under contract No. DE-AC03-76SF00098.

FIGURE CAPTIONS

Fig.1 Schematic diagram of the STM experiment. A piezoelectric tube supports a sharp tip and displaces it over the surface at a distance of a few Angstroms. The tunnel current is measured and maintained constant during scanning by means of an electronic feedback. The images are generated by plotting the xy and z displacements of the tip.

Fig.2 Current image of a 10x10 Å area of a Pt(111) surface that is covered by a monolayer of graphitized carbon. The higher tunnel current is found over the C-C bonds.

Fig.3 Image of a Mo(001) surface that is covered by a monolayer of Sulfur. The unit cell of the S structure is marked by the rectangle and contains two S atoms. The S-S distance is 3.1 Å. The image is taken in air and the Mo surface is protected from oxidation by the saturation monolayer of S.

Fig.4 1000x1000 Å image of a surface of Mo(001) that has oxidized after exposure to air for three days. The S overlayer has been displaced. The oxide crystallites are oriented along the [001] and [010] directions. Corrugation is approximately 20 Å.

Fig.5 A 100x100 Å current image of a Re(0001) surface covered by S with a coverage between 0.25 and 0.3. The structure is mostly (2x2) sprinkled with numerous trimers. Trimers form preferentially near domain boundaries and appear brighter that the (2x2) region. Notice also that all trimers have the same orientation.

Fig.6 Topographic 100x100 Å image of a Re(0001) surface saturated with trimers. An ordered $(3\sqrt{3}x3\sqrt{3})R30^\circ$ structure is formed. Notice that 1/4 of the trimers have a different orientation. Some point defects are also observed. Vertical gray scale = 2 Å

Fig.7 68x68 Å Current image showing the tetrameres of S formed at coverage above 0.45. Notice the asymmetry of the intensity of the S atoms that reflect the symmetry of the unit cell with only one mirror plane across the long diagonal in the diamond shaped tetrameres.

Fig.8 Topographic image of the $(2\sqrt{3}x2\sqrt{3})R30^\circ$ structure showing the aggregation of S into hexagonal units. The distance between centers of adjacent hexagons is approximately 9 Å. A step separates two terraces and produces the blurred region of the image. Notice also numerous defects and domain boundaries.

REFERENCES

[1] G. Binnig, H. Rohrer, Ch. Gerber and E. Weibel. Phys. Rev. Lett. 49, 57 (1982).

[2] M.A. Van Hove and S.Y. Tong, *Surface Crystallography by LEED.* Springer Series in Chemical Physics 2. Berlin. 1979.

[3] G.A. Somorjai. *Chemistry in Two Dimensions: Surfaces.* Cornell University Press. Ithaca. New York. 1981.

[4] M. Salmeron. *Emerging Techniques for Catalyst Characterization.* Chapter 5. Edited by Catalytica. Mountain View. CA. 1989.

[5] Y. Kuk and P.J. Silverman, Rev. of Sci. Instr. 60, 165 (1986).

[6] M. Salmeron, G.A. Somorjai and R.R. Chianelli, Surf. Sci. 127, 526 (1983).

[7] A. Gellman, W.T. Tysoe, F. Zaera and G.A. Somorjai, Surf. Sci. 191, 271 (1987).

[8] B. Marchon, P. Bernhardt, M.E. Bussell, G.A. Somorjai, M. Salmeron and W. Siekhaus, Phys. Rev. Lett. 60, 1166 (1988).

[9] B. Marchon, D.F. Ogletree, M.E. Bussell, G.A. Somorjai, M. Salmeron and W. Siekhaus, J. of Microsc. 152, 427 (1988).

[10] D.G. Kelly, A.J. Gellman, M. Salmeron, G.A. Somorjai, V. Maurice and J. Oudar, Surf. Sci. 204, 1 (1988).

[11] D.F. Ogletree, C. Ocal, B. Marchon, G.A. Somorjai and M. Salmeron, J. Vac. Sci. Technol. A8, 297 (1990).

[12] R.Q. Hwang, D.M. Zeglinski, A. López Vázquez-de-Parga, C. Ocal, D.F. Ogletree, G.A. Somorjai, M. Salmeron and D.R. Denley, Phys. Rev. Lett. (submitted).

[13] D.F. Ogletree, R.Q. Hwang, D.M. Zeglinski, A. López Vázquez-de-Parga, G.A. Somorjai and M. Salmeron. J. Vac. Sci. Technol. A, (in press).

[14] H. Ohtani, C.-T. Kao, M.A. Van Hove and G.A. Somorjai, Progress in Surface Science, 23, 155 (1986).

[15] M.A. Van Hove, S.W. Wang, D.F. Ogletree and G.A. Somorjai, Advances in Quantum Chemistry, 20, 1 (1989).

[16] T.L. Einstein, Surf. Sci., L497 (1979).

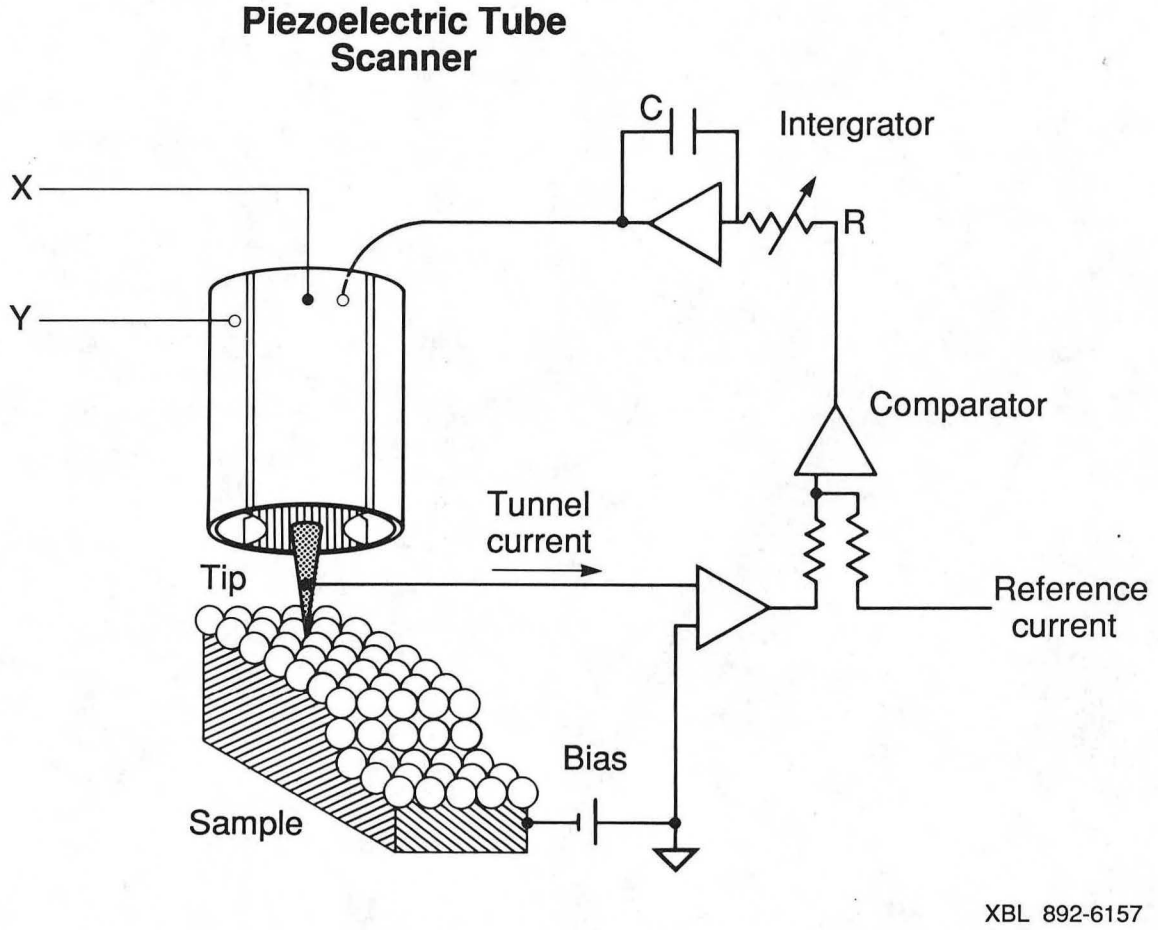
Piezoelectric Tube Scanner
C
Intergrator
X
R
Y
Comparator
Tunnel current
Tip
Reference current
Bias
Sample
XBL 892-6157

Fig. 1

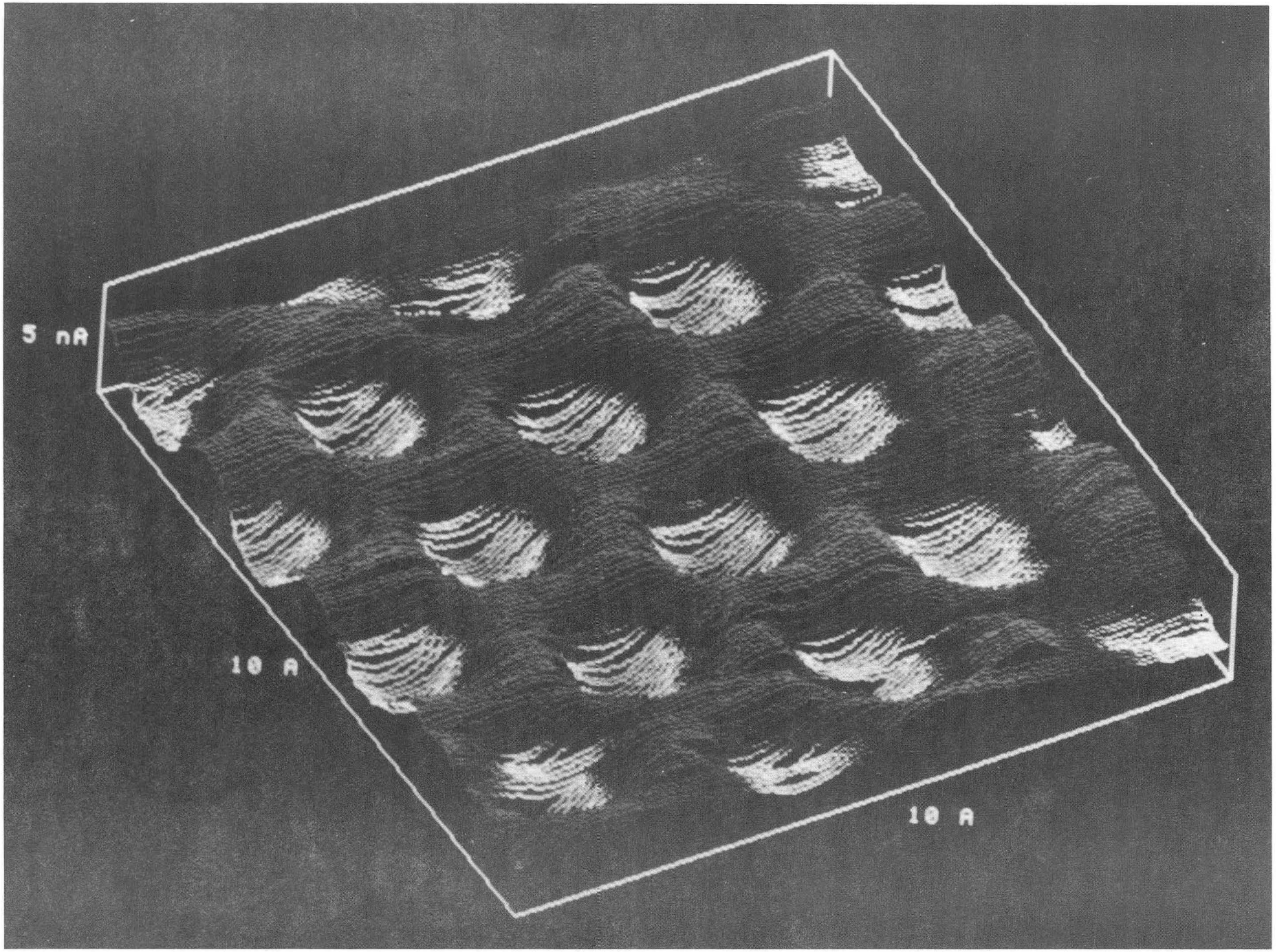

Fig. 2

CBB 882-849

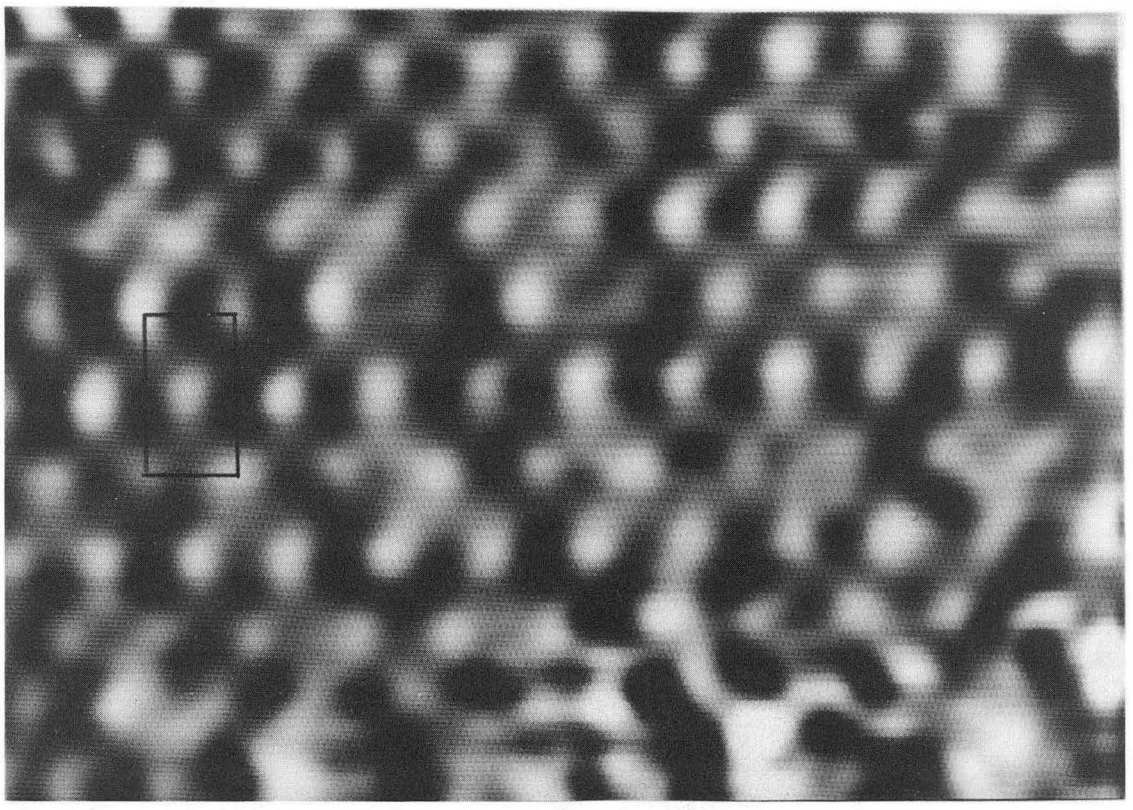

XBB 870-9763

Fig. 3

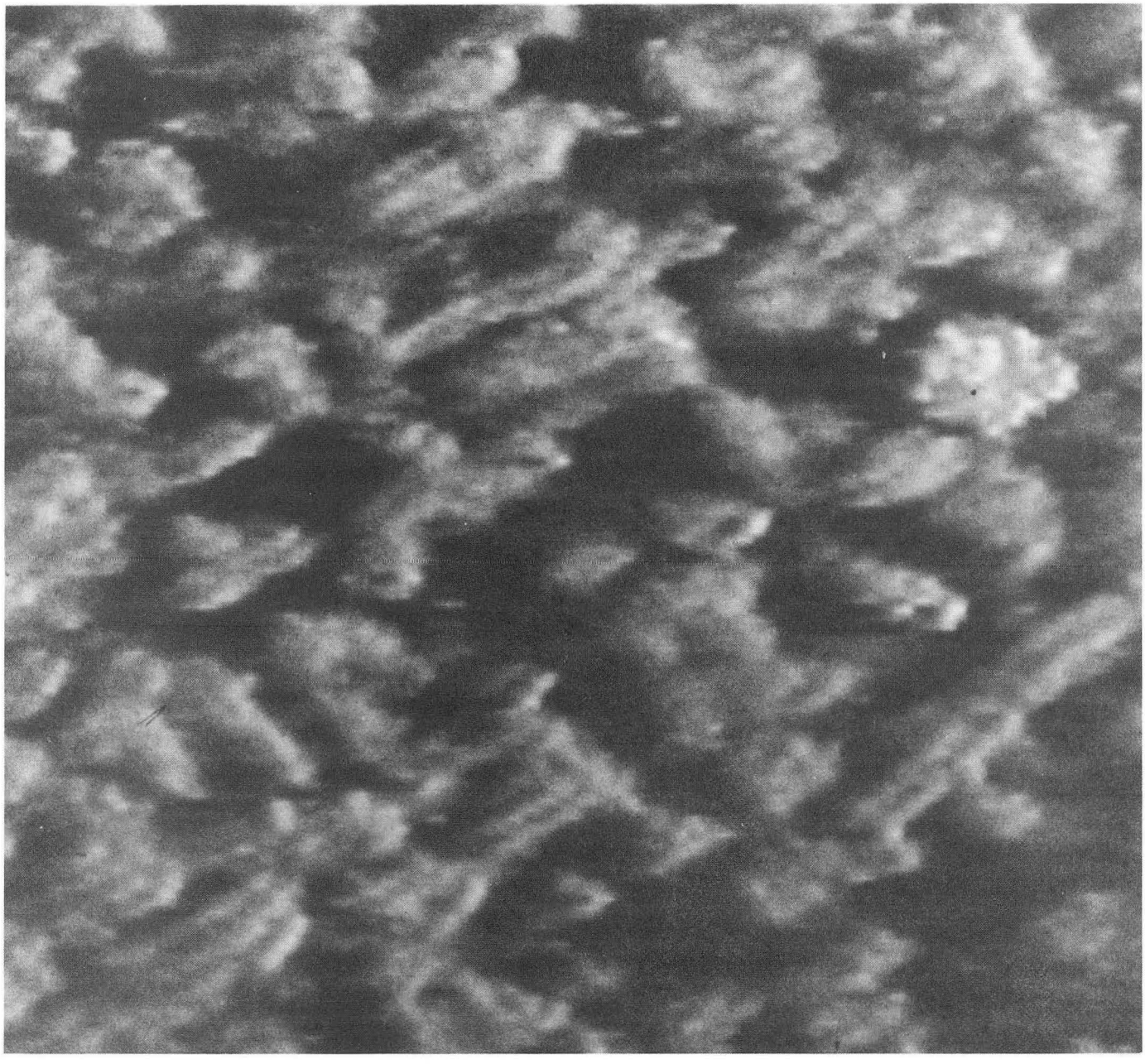

XBB 886-6471

Fig. 4

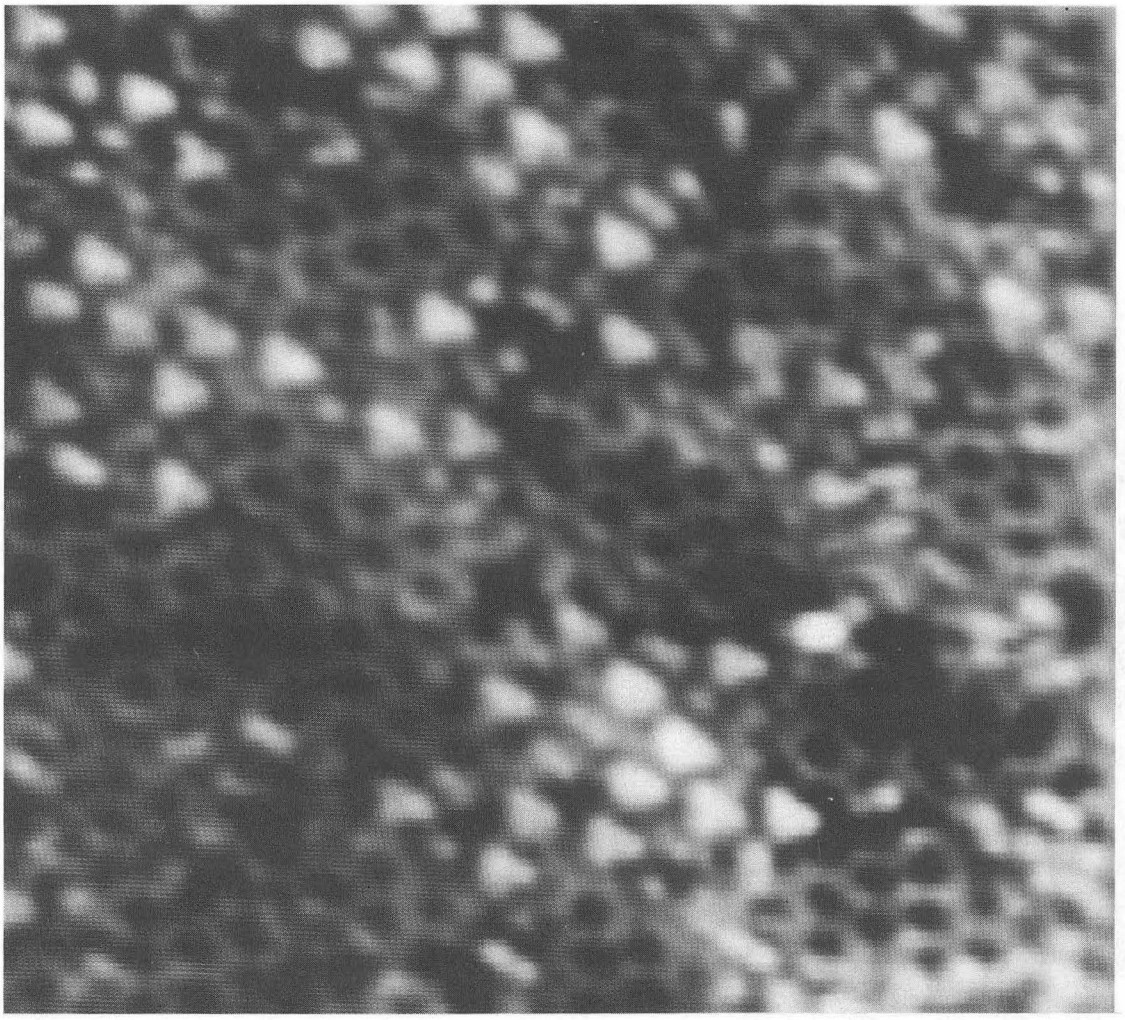

XBB 906-5048

Fig. 5

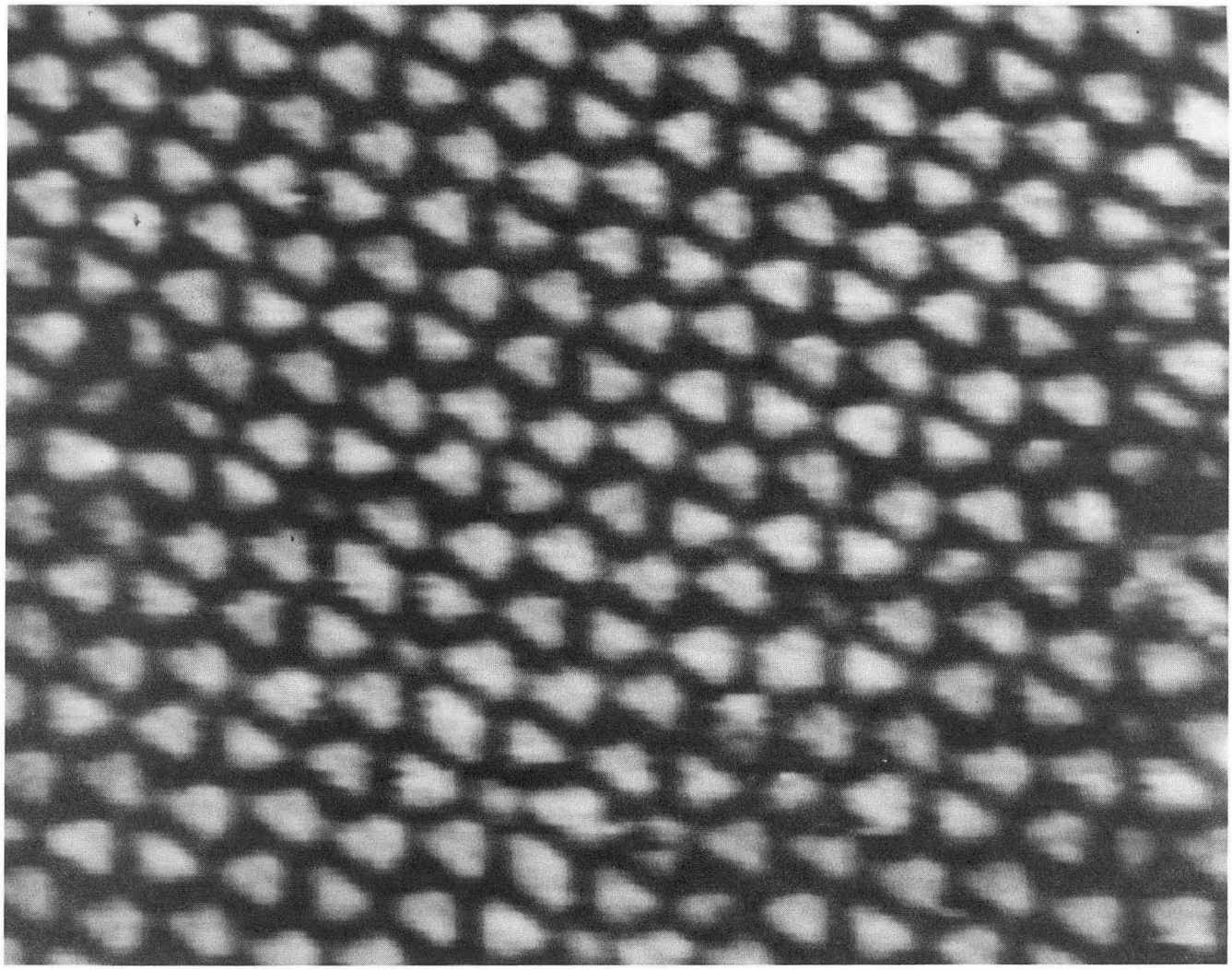

XBB 907-5511

Fig. 6

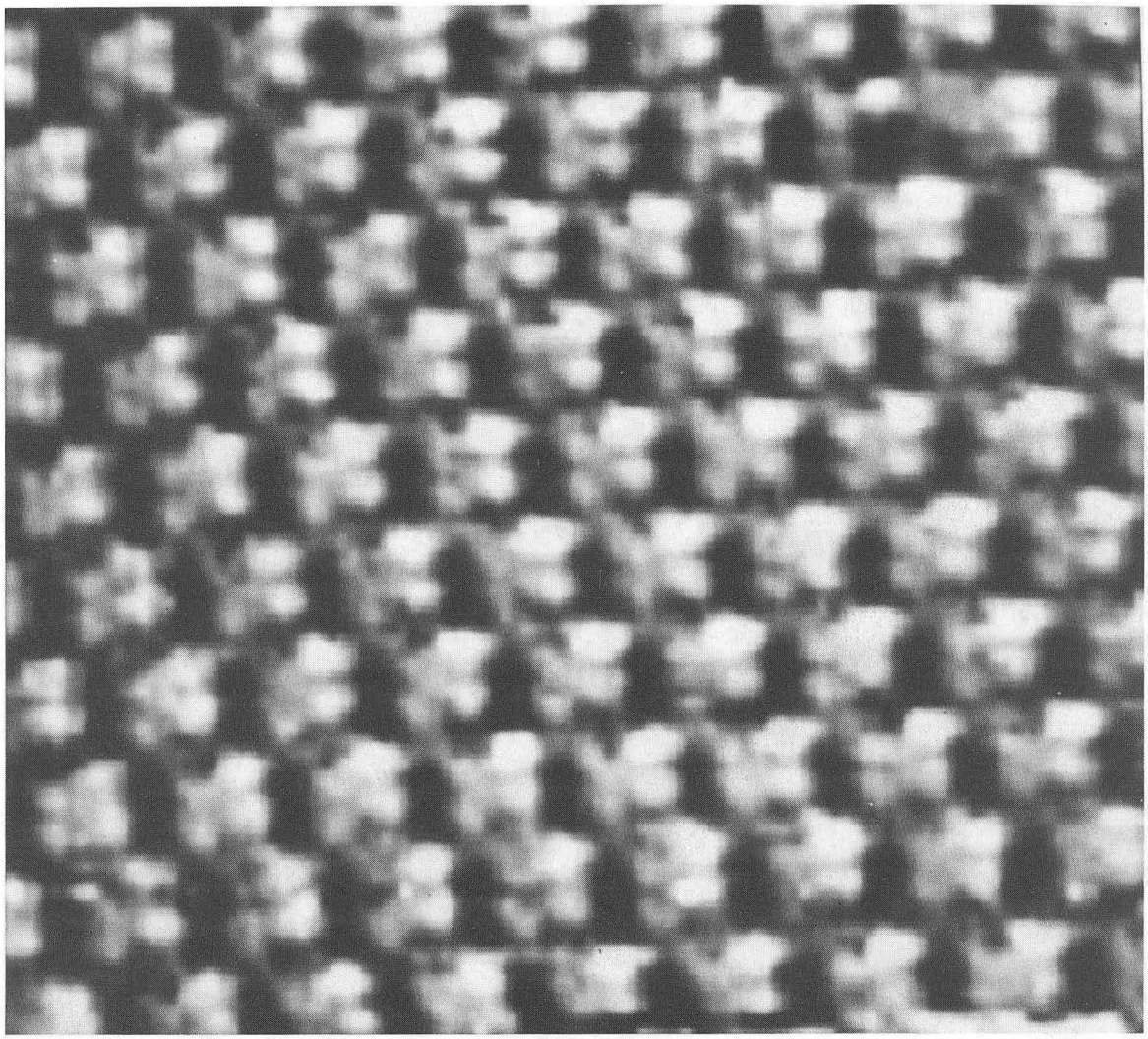

XBB 907-5508

Fig. 7

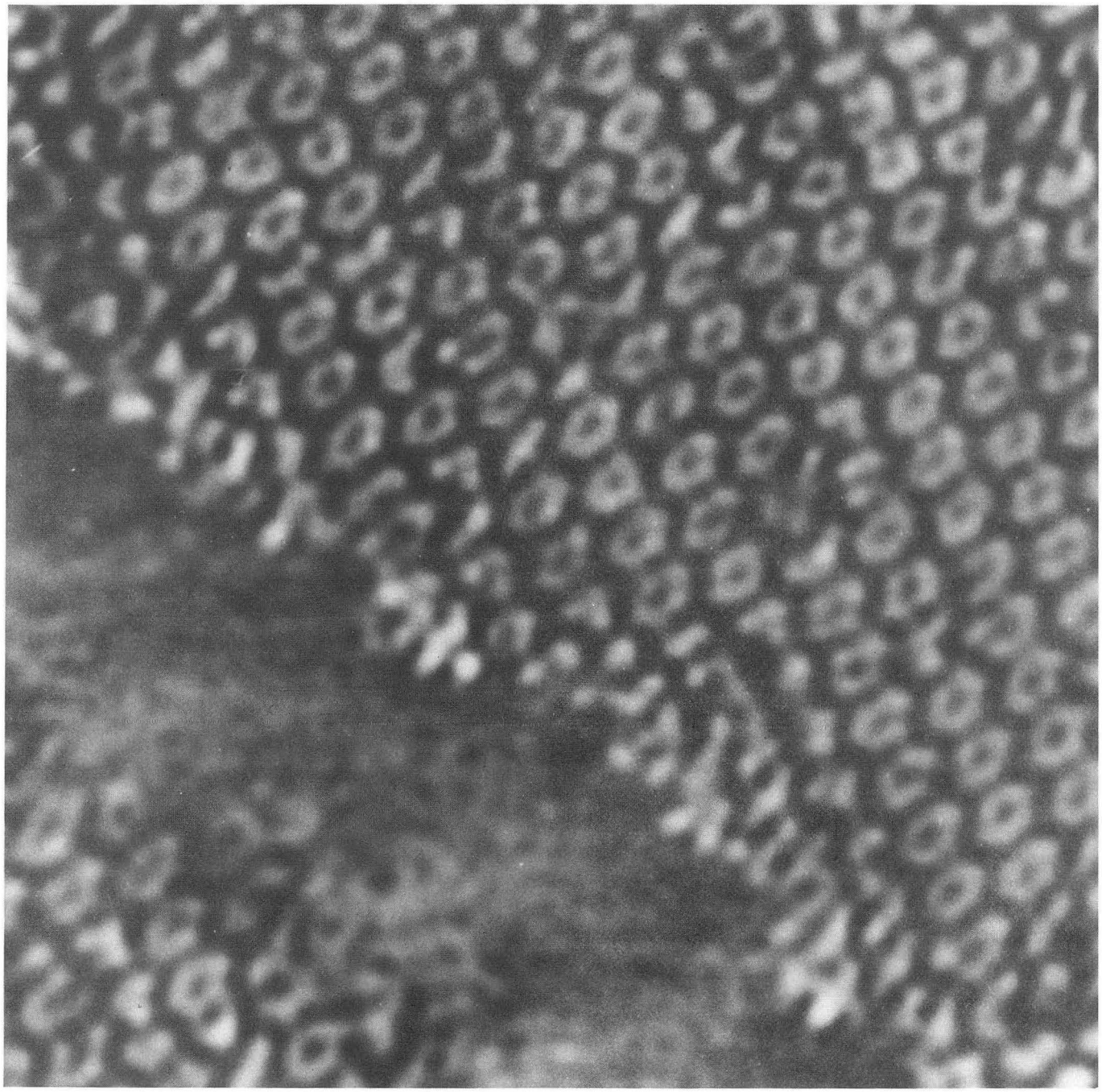

XBB 888-8469

Fig. 8

LAWRENCE BERKELEY LABORATORY
CENTER FOR ADVANCED MATERIALS
1 CYCLOTRON ROAD
BERKELEY, CALIFORNIA 94720